

STUDY OF RELATIVISTIC FORWARD-BACKWARD HADRON
PRODUCTION IN THE INTERACTIONS OF ^3He AND ^4He WITH
EMULSION NUCLEI AT DUBNA ENERGY

A. ABDELSALAM^a, M. S. EL-NAGDY^b, E. A. SHAAT^a, N. ALI-MOSSA^c,
O. M. OSMAN^a, Z. ABOU-MOUSSA^a, S. KAMEL^{d,1}, N. RASHED^e, W. OSMAN^a,
M. E. HAFIZ^d, B. M. BADAWY^f and S. MAGD ELDIN^a

^a*Physics Department, Faculty of Science, Cairo University, Egypt*

^b*Physics Department, Faculty of Science, Helwan University, Cairo, Egypt*

^c*Basic Science Department, Faculty of Engineering, Zagazig University, Shoubra, Egypt*

^d*Physics Department, Faculty of Education, Ain Shams University, Cairo, Egypt*

^e*Physics Department, Faculty of Science, Cairo University, El-Fayom Branch, Egypt*

^f*Reactor Physics Department, Nuclear Research Center, Atomic Energy Authority Egypt*

Received 31 January 2004; Accepted 6 June 2006

Online 10 November 2006

The experimental results on ^3He - and ^4He -emulsion interactions accompanied by relativistic (shower) hadrons flying into the backward ($\theta_{\text{lab}} \leq 90^\circ$) hemisphere at 4.5 AGeV/c are presented and analyzed. The dependence of the probabilities of these interactions on the different target sizes, impact parameter and projectile spectator charges is studied. An investigation of average values and multiplicity distributions of these hadrons for the interactions with light and heavy emulsion nuclei has been carried out. In addition, the correlations between the multiplicities of different types of the emitted particles are studied. The data show that backward shower particles are a sensitive target parameter. The values of impact parameters can be used as good indicators for selecting events which occurred with light or heavy emulsion nuclei. A comparison with the modified cascade model shows a good performance in describing the data produced in the region having less cascading (i.e. interactions with light nuclei). As for the interactions with heavy nuclei, the model overestimates the experimental data.

PACS numbers: 25.75.-q, 25.55.-e,

UDC 539.172

Keywords: ^3He - and ^4He -emulsion interactions, backward shower particles, multiplicity distributions, modified cascade model

¹Corresponding author, E-mail address: sayedks@hotmail.com

1. Introduction

In the last few years, the phenomena of backward relativistic particle emission in hadron-nucleus and nucleus-nucleus interactions at high energies have attracted much attention from both the theoretical and experimental points of view [1–13]. A principal reason for studying the production of relativistic hadrons from nuclei in the backward hemisphere (BHS) is that such production is kinematically restricted in free nucleon-nucleon collisions. The emission of the relativistic hadrons beyond the kinematic limits may then be an evidence for exotic production mechanisms such as production from clusters [2, 6, 14, 15]. In early experimental publications at Dubna, the authors [1] argued that the simple Fermi motion could not account for the production of backward hadrons, and stated that the dominant mechanism for emission of such hadrons was an interaction between incident nucleons and multi-nucleon clusters in the target, referring to this mechanism as cumulative production. In the LBL experiments at Bevatron [5], the backward pion production data supported a model called the “effective target model” [9], where the incident nucleons are assumed to interact with the row of nucleons along its paths and excite them in a collective fashion. During the de-excitation, relativistic pions are emitted as in the thermal models.

The present work is complementary to our program [10–13] of studying the characteristics of the backward particle production in the interactions of various projectiles with emulsion nuclei at Dubna energy. Here, the general characteristics of the backward shower particles are compared with those of the corresponding forward ones induced in the interactions of 3.7 AGeV ^3He and ^4He isotopes with emulsion nuclei. The present experimental data are analyzed in the framework of the predictions of the modified cascade model (MCM) [16, 17].

2. Description of the basic model

According to the modified cascade model (MCM), when one of the projectile nucleons interacts with one of the target nucleons, creation of a new particle takes place. The participating target nucleon acquires momentum and begins to move in the nucleus. Such moving (cascade) particles can interact with other target/projectile nucleons to produce new particles or suffer elastic rescattering. The nucleons, which can participate in elementary interactions, are chosen randomly from the initial configuration system. All nucleons of the colliding nuclei with mass numbers A and B are identified by the coordinates $(x_i, y_i, z_i, i = 1, \dots, A)$ and $(x_j, y_j, z_j, j = 1, \dots, B)$ in the initial configuration state. Taking into account the Lorentz contraction of the projectile nucleus A in the rest frame of the target nucleus B , the corresponding coordinates are redefined as $z_i \rightarrow z_i/\gamma - R_A/\gamma - R_B$, where γ is the Lorentz factor of the projectile nucleus and R_A (R_B) are the radii of the nuclei. Nucleons whose coordinates satisfy the condition

$$(b_x + x_i - x_j)^2 + (b_y + y_i - y_j)^2 \leq (R_{\text{int}} + \Lambda_D)^2$$

are considered to participate in the elementary interactions, where (b_x, b_y) are the components of the impact parameter vector, R_{int} is the strong interaction radius (~ 1.3 fm) and Λ_D is the de Broglie wavelength of the projectile nucleon. The time evolution of the system is determined by considering many independent simulations of the collision process, and taking average over the values of those quantities calculated in each run. All collisions that take place in the closest time interval are independently processed. A nucleon involved in the interaction is treated as a cascade particle as soon as it undergoes its first interaction.

The momenta of the colliding particles are determined randomly according to the differential cross section. After the first nucleon-nucleon collision has been completed, straight-line motion is resumed and the next possible collision is followed in a similar manner and so on. The process continues until all moving particles either escape from the nucleus or are absorbed. At the end of the fast cascade stage of the process, the number and charges of spectator nucleons, as well as the charges of the absorbed mesons, determine the nuclear residual mass number and charge.

The excitation energy of the nuclear residual is the sum of the energies of absorbed particles (cascade nucleons) and the holes (the participating nucleons) counted from the Fermi energy. In addition, Pauli exclusion principle and the energy-momentum conservation are obeyed in each intra-nucleon interaction. In addition, the trailing effect (rearranging the density) is included: a target nucleon is scattered because of collision with the projectile, and the whole target density is depleted by one nucleon.

The model overestimates the meson production, and several efforts were done to overcome the problem. Kawrakow et al. [18] introduced the concept of the formation time of secondary particles. It is assumed that, during the time required for the formation of a self-mesonic cloud, product particles cannot interact. The formation time, which depends on hadron properties, is considered as a free parameter and the problem is reduced to the choosing of this parameter.

Generated events consisting of 5000 interactions are simulated for each projectile-target combination using the code developed by Barashenkov et al. [19].

It should be noted that a similar realization of the above model was recognized as the best model applied for the interaction of small projectiles with heavy nuclei in the intermediate energy range (1–10) AGeV [20, 21]. As seen from Table 1, the

TABLE 1. Experimental mean values of total shower particles in A A collisions at about 4.5 AGeV/c, compared with those predicted by MCM calculations.

	³ He 4.5 AGeV/c	⁴ He 4.5 AGeV/c	¹² C 4.5 AGeV/c	¹⁶ O 4.5 AGeV/c	²² Ne 4.1 AGeV/c	³² S 4.5 AGeV/c
Exp.	4.0 ± 0.1	4.5 ± 0.1	9.5 ± 0.2	12.2 ± 0.2	11.7 ± 0.7	16.4 ± 0.6
MCM	3.59	4.50	9.44	11.27	11.90	16.00
Ref.	Present work	Present work	[16]	[16]	[16]	[16]

model fairly well describes the measured mean values of the total shower particles in A-A interaction at (4.1–4.5) AGeV/c (given in Ref. 16), as well as those of helium isotopes measured in the present work.

3. Experimental details

Two stacks of NIKFI-BR2 nuclear emulsion with dimensions of 10 cm × 20 cm × 600 μm were irradiated by ³He and ⁴He beams with momentum of 4.5 AGeV/c at Dubna/JINR synchrophasotron. The chemical compositions of this emulsion type [13] are hydrogen (39.54%), carbon (17.70%), nitrogen (4.96%), oxygen (12.00%), bromine (12.90%) and silver (12.90%). The percentage given for each element is the weight of nuclei in the used emulsion. Along the track, double scanning, fast in the forward direction and slow in the backward one, was carried out using a total magnification of about 1500×. Data studied in the present work consist of 1796 and 1161 total interactions of ³He and ⁴He projectiles with emulsion (Em) nuclei, respectively. These are collected from a respective total scanned length of 332.6 m and 217.6 m. The events due to the electromagnetic dissociation and elastic scattering are rejected from the used samples. The remaining unbiased samples of 1685 and 1092 inelastic interactions, indicate mean free paths λ_{inel} equal 19.74 ± 0.48 cm, and 19.93 ± 0.60 cm for inelastic interactions of ³He+Em and ⁴He+Em, respectively.

The tracks of the emitted secondary charged particles in each event were classified according to the traditional emulsion criteria as follows:

a) Shower tracks (s) are singly charged relativistic particles with relative ionization $I/I_0 \leq 1.4$ where I is the track ionization and I_0 is the plateau ionization for singly charged minimum ionizing particles. Their multiplicity is denoted by n_s .

b) Grey tracks (g) have range $L \geq 3$ mm in emulsion and relative ionization $I/I_0 \geq 1.4$. These tracks are mostly due to protons of kinetic energy in the range 26–400 MeV. Their multiplicity is denoted by N_g .

c) Black tracks (b) are those having range of $L < 3$ mm, corresponding to protons with kinetic energy ≤ 26 MeV. They are mainly due to evaporated target fragments. Their multiplicity is denoted by N_b . In each event, the black and grey tracks together are called highly ionizing tracks. Their multiplicity is denoted by ($N_h = N_g + N_b$).

d) Projectile fragments (PFs), emitted with an angle $\theta \leq 3^\circ$ (where θ is the emission angle with respect to the beam axis), are characterized by no change in their ionization for at least 2 cm from the interaction point. In the present case, they are singly and doubly charged particles, spectator (stripped) fragments of the projectile nucleus, having velocity $v \simeq 0.97 c$. The total charge of the stripped fragments in the forward cone per event is denoted by Q . The singly-charged fragments emitted in the fragmentation cone were subjected to rigorous multiple scattering measurements for the momentum determination in order to separate the produced pions from the singly charged fragments.

For the present analysis, the produced particles in each event are divided into

particles emitted in the forward hemisphere (FHS) of the reaction ($\theta < 90^\circ$) and particles emitted in the backward hemisphere (BHS) ($\theta \geq 90^\circ$).

4. Experimental results and model predictions

4.1. Target separation

Since the emulsion is a composite target, the incident nucleus (${}^3\text{He}$ or ${}^4\text{He}$) will interact with one of the following groups of target nuclei: the free hydrogen (H), light (C, N, O) and heavy (Ag, Br) nuclei, of average atomic weights 1, 14 and 94, respectively. Following the method described in detail in Refs. [22] and [23], the number of collisions belonging to each group is chosen statistically. Accordingly, the numbers of inelastic interactions of ${}^3\text{He}$ projectile with the three groups of nuclei (H, CNO and AgBr) are 118 (7%), 472 (28%) and 1095 (65%) and those induced by ${}^4\text{He}$ one are 55 (5%), 327 (30%) and 710(65%), respectively. However, we analyzed the interactions of the beams of ${}^3\text{He}$ and ${}^4\text{He}$ with the two main parts of emulsion nuclei, the light nuclei (C, N, O) and the heavy ones (Ag, Br), which are characterized by the total charge of different stripped projectiles $Q = 0$ and ≥ 1 , and by different impact parameters $N_h \leq 8$ and $N_h > 8$.

4.2. Probabilities of the shower particle production in BHS

Table 2 illustrates the probabilities of observing events having at least one shower particle ($p(n_S^b > 0)$) flying into BHS in ${}^3\text{He}+\text{Em}$ and ${}^4\text{He}+\text{Em}$ interactions at 3.7 AGeV. The probabilities of these events for different target sizes (CNO and AgBr) and different groups of events ($N_h \leq 8$, $N_h > 8$ and $Q = 0$ and ≥ 1) are presented. The table shows that the probabilities $p(n_S^b > 0)$ follow a similar behavior for the events induced by ${}^3\text{He}$ and by ${}^4\text{He}$ nuclei. Also, a slight increase of $p(n_S^b > 0)$ can be seen when transiting from events produced by ${}^3\text{He}$ to those produced by ${}^4\text{He}$ for different target sizes (CNO, Em and AgBr), and different impact parameters ($N_h \leq 8$ and $N_h > 8$). This may be due to the increase in the projectile mass, which leads to an increase in the number of interacting projectile nucleons. Also, for both interactions, the value of $p(n_S^b > 0)$ for events having $N_h > 8$

TABLE 2. The percentage probabilities of the present interactions accompanied by shower particles emitted in the BHS at different target sizes, impact parameters and stripped projectiles. The corresponding MCM results are given in parentheses.

Projectile	CNO	Em	AgBr	$N_h \leq 8$	$N_h > 8$	$Q = 0$	$Q \geq 1$
${}^3\text{He}$	12.3	23.3	29.2	12.3	42.6	37.7	15.7
	(14.38)	(27.62)	(35.82)	(16.15)	(60.32)	(36.83)	(16.08)
${}^4\text{He}$	16.2	26.5	32.0	16.3	50.2	37.7	20.0
	(15.57)	(29.44)	(38.09)	(17.55)	(62.58)	(40.25)	(17.88)

(group of events belongs to AgBr nuclei) is three times larger than the corresponding value for events having $N_h \leq 8$ (i.e. those belonging to CNO nuclei and peripheral collisions with AgBr nuclei). The dependence of $p(n_S^b > 0)$ on the projectile spectator charge Q is represented in Table 2 for different channels ($Q = 0$ and ≥ 1). It should be noted that the value of forward spectator charge Q , characterizing the degree of centrality, is related to the interaction impact parameter [10–13]. Interactions having $Q = 0$ are due to the central collisions, while those with $Q \geq 1$ represent the peripheral collisions. As one can expect, there is a significant decrease of $p(n_S^b > 0)$ as the impact parameter increases. The theoretical calculations performed in the framework of the MCM, presented in parentheses in Table 2, are in qualitative agreement with our experimental data for the interactions of ^3He and ^4He with light nuclei. However, the MCM calculations overestimate the corresponding experimental data for heavy nuclei.

4.3. Multiplicities of shower particles in FHS and BHS

Table 3 presents the average multiplicities of the shower particles emitted in both FHS and BHS, $\langle n_S^{f,b} \rangle$, for all obtained samples, and for events having $n_S^b > 0$ in interactions of $^3\text{He}+\text{Em}$ and $^4\text{He}+\text{Em}$ at 3.7 AGeV, as well as for the interactions

TABLE 3. The values of the average forward and backward multiplicities of the emitted shower particles for different emulsion targets, as well as for events having $n_S^b > 0$. $(F/B)_S$ is the forward - backward ratio. The corresponding MCM results are given in parentheses.

	Target	$\langle n_S^f \rangle$	$\langle n_S^b \rangle$	$(F/B)_S$
^3He	Em ($n_S^b > 0$)	5.09 ± 0.16 (5.11)	1.22 ± 0.02 (1.97)	4.17 (2.59)
	CNO	2.63 ± 0.07 (2.41)	0.13 ± 0.01 (0.16)	20.20 (15.06)
	Em	3.68 ± 0.07 (3.21)	0.29 ± 0.01 (0.38)	12.70 (8.45)
	AgBr	5.31 ± 0.12 (3.74)	0.53 ± 0.03 (0.51)	10.02 (7.33)
^4He	Em ($n_S^b > 0$)	5.98 ± 0.21 (6.52)	1.32 ± 0.04 (2.04)	4.53 (3.20)
	CNO	2.97 ± 0.09 (2.97)	0.17 ± 0.02 (0.17)	17.47 (17.47)
	Em	4.19 ± 0.10 (4.08)	0.35 ± 0.02 (0.42)	11.97 (9.71)
	AgBr	6.70 ± 0.18 (4.82)	0.71 ± 0.05 (0.57)	9.44 (8.46)

with different targets (CNO and AgBr). This table shows the corresponding results of the MCM calculations in parentheses. The values of $\langle n_S^{f,b} \rangle$ obtained for different impact parameters ($N_h \leq 8$ and $N_h > 8$) and different Q 's ($Q = 0$ and ≥ 1) are presented in Table 4. The forward to backward ratios for shower particles, $(F/B)_S$ are displayed in Tables 3 and 4 for the presented data. From these two tables, one can conclude that:

i) The values of $\langle n_S^f \rangle$ for different target sizes and different impact parameters are higher than the corresponding ones of $\langle n_S^b \rangle$. For the considered different targets, both average values $\langle n_S^{f,b} \rangle$ increase slightly from ${}^3\text{He}$ to ${}^4\text{He}$.

ii) For each of the two projectiles, the values of $\langle n_S^b \rangle$ show a stronger dependence on the target size than do the values of $\langle n_S^f \rangle$. This comes from the observation that the ratio $\langle n_S^b \rangle_{\text{AgBr}} / \langle n_S^b \rangle_{\text{CNO}}$ is nearly twice the corresponding ratio for $\langle n_S^f \rangle$.

iii) The mean values of the shower particles produced in the two hemispheres increase when going towards centrality, i.e., as the impact parameter decreases (indicated by either the increase of N_h value or the decrease of the Q value).

iv) The group of events accompanied by the backward emission of shower particles ($n_S^b > 0$) [393 (23.3%) and 289 (26.5%) for ${}^3\text{He} + \text{Em}$ and ${}^4\text{He} + \text{Em}$, respec-

TABLE 4. The values of $\langle n_S^f \rangle$, $\langle n_S^b \rangle$ and $(F/B)_S$ ratio for different N_h - values and different stripped projectiles due to ${}^3\text{He} + \text{Em}$ and ${}^4\text{He} + \text{Em}$ interactions. The corresponding MCM results are given in parentheses.

Interaction group		$\langle n_S^f \rangle$	$\langle n_S^b \rangle$	$(F/B)_S$
${}^3\text{He}$	$N_h \leq 8$	2.80 ± 0.07 (2.70)	0.13 ± 0.01 (0.40)	21.54 (8.71)
	$N_h > 8$	5.44 ± 0.12 (6.35)	0.55 ± 0.03 (1.73)	9.89 (3.67)
	$Q = 0$	5.51 ± 0.12 (4.69)	0.47 ± 0.03 (1.01)	11.72 (4.64)
	$Q \geq 1$	2.71 ± 0.05 (2.34)	0.19 ± 0.01 (0.42)	14.26 (5.57)
${}^4\text{He}$	$N_h \leq 8$	3.02 ± 0.09 (3.21)	0.18 ± 0.02 (0.40)	16.78 (8.03)
	$N_h > 8$	6.91 ± 0.19 (8.28)	0.74 ± 0.05 (1.85)	9.34 (4.48)
	$Q = 0$	6.34 ± 0.17 (6.19)	0.54 ± 0.04 (1.10)	11.74 (5.63)
	$Q \geq 1$	2.96 ± 0.09 (2.79)	0.24 ± 0.02 (0.44)	12.33 (6.34)

tively], Table 3, are characterized by high values of $\langle n_S^{f,b} \rangle$. In this case, for both projectiles, the value of $\langle n_S^b \rangle$ is about twice the total sample highest value (that for AgBr). On the other hand, the value of $\langle n_S^f \rangle$ for the events having $n_S^b > 0$ is just nearly equal the total sample value obtained with AgBr.

v) The $(F/B)_S$ ratio decreases rapidly with increasing target size (from CNO to AgBr, as well as from $N_h \leq 8$, to $N_h > 8$ groups). Concerning the dependence of $(F/B)_S$ ratio on the mass number of helium, one observes that, while for the interactions with light (CNO) nuclei the ratio $(F/B)_S$ decreases from ${}^3\text{He}$ to ${}^4\text{He}$, that ratio when heavy (AgBr) nuclei are the target shows a possible limiting behavior. Such limiting behavior is also noticed when the events with $n_S^b > 0$ are considered.

vi) Results of MCM calculations shown in Table 3 for both $\langle n_S^{f,b} \rangle$ are in a qualitative agreement with the existing data for the interactions with the light (CNO) nuclei. As for the interactions with the heavy (AgBr) nuclei, the MCM calculations generally underestimate the measured results.

In addition to the previous experimental results, it has been noticed that when the samples of events having $N_h \leq 8$ and $n_S^b > 0$ are considered for the interactions of ${}^3\text{He}+\text{Em}$ and ${}^4\text{He}+\text{Em}$, the obtained values of $\langle n_S^b \rangle$ are equal to 1.08 ± 0.09 and 1.11 ± 0.10 , respectively. These results are found to be in agreement with the values of $\langle n_S^b \rangle$ which are presently determined for events due to interactions of ${}^3\text{He}+\text{CNO}$ (1.07 ± 0.14) and of ${}^4\text{He}+\text{CNO}$ (1.09 ± 0.02). On the other hand, the values of $\langle n_S^b \rangle$ for the events with $N_h > 8$ and $n_S^b > 0$ are found to be 1.30 ± 0.08 for ${}^3\text{He}$ and 1.48 ± 0.12 for ${}^4\text{He}$. The corresponding values of $\langle n_S^b \rangle$, calculated for collisions with AgBr nuclei, are 1.25 ± 0.07 and 1.38 ± 0.09 . This illustrates that, for both projectiles, the events having $N_h \leq 8$ and $n_S^b > 0$ can be considered as indicators of interactions with the light emulsion nuclei, while those with $N_h > 8$ and $n_S^b > 0$ point to the quasicentral and central interactions with the heavy emulsion nuclei.

4.4. Multiplicity distributions of forward and backward shower particles

It has been noticed earlier [10–12] that particles produced in the BHS region are closely related with the target fragmentation region, i.e., with that part of phase space where all single-particle characteristics are most certainly independent of the projectile size. In this section, we compare the experimental multiplicities of shower particles emitted in FHS, $p(n_S^f)$, and BHS, $p(n_S^b)$, for the interactions studied in this work with the corresponding theoretical predictions of the MCM.

Figures 1a, b and c represent the multiplicity distributions $p(n_S^f)$ for the interactions of two helium isotopes with CNO, Em and AgBr nuclei, respectively. The corresponding distributions $p(n_S^b)$ are shown in Figs. 2a, b and c. The theoretical predictions according to MCM are also presented in these two figures as histograms.

a) $p(n_S^f)$ distributions: In Fig. 1a is seen that the experimental multiplicity

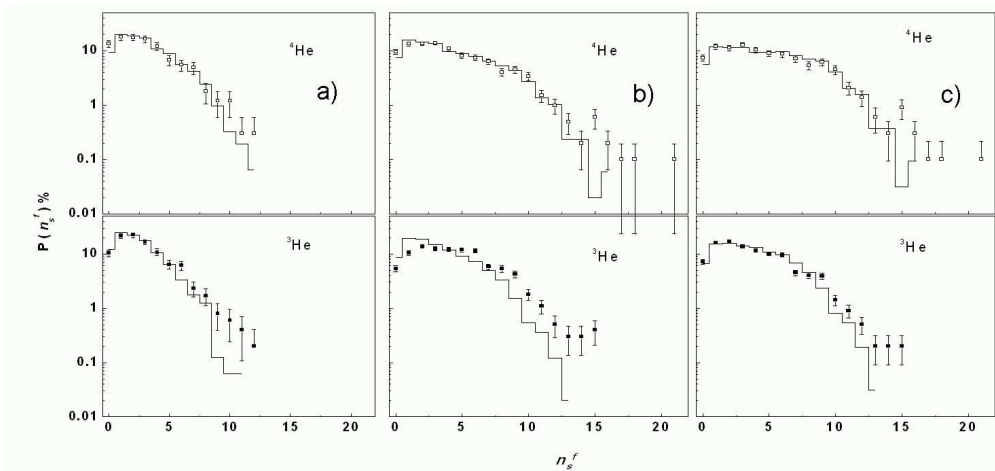


Fig. 1. (a, b and c): Experimental multiplicity distributions (error bars) of forward shower particles, $p(n_s^f)$, in the interactions of ${}^3\text{He}$ and ${}^4\text{He}$ with CNO (a), Em (b) and AgBr (c) nuclei at 3.7 AGeV, respectively, together with the theoretical calculations of MCM (histograms).

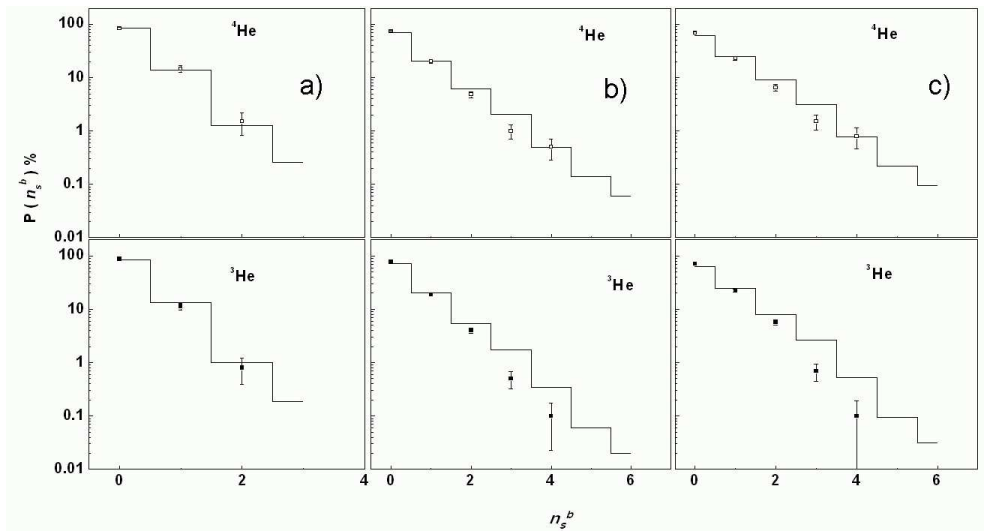


Fig. 2. (a, b and c): Experimental multiplicity distributions (error bars) of backward shower particles, $p(n_s^b)$, in the interactions of the two helium isotopes with CNO (a), Em (b) and AgBr (c) nuclei. The notations are the same as in Fig. 1.

distributions of the relativistic shower particles of ${}^3\text{He}+\text{CNO}$ and ${}^4\text{He}+\text{CNO}$ interactions are well described by the MCM calculations, except for high multiplicity tails, where the model underestimates the experimental results. Considering the

interactions with Em and AgBr, the experimental $p(n_S^f)$ distributions of ^4He interactions in Fig. 1b and c extend to greater n_S^f -values than do the corresponding distributions of ^3He . This may be attributed to a difference in the total incident energy and/or in the structure of the two helium isotopes. As one can see, the n_S^f ranges covered by the MCM calculations for ^4He distributions ($n_S^f \leq 14$) are larger than those for ^3He ($n_S^f \leq 9$). Consequently, it can be concluded that the best agreement between the experimental data and the theoretical predictions is achieved for the two helium isotopes when they interact with the light group of nuclei (CNO). This conclusion is compatible with the experimental and theoretical data $\langle n_S^f \rangle$ presented in Table 3.

b) $p(\mathbf{n}_S^b)$ distributions: In Figs. 2a, b and c, the experimental multiplicity distributions of the shower particles emitted in the BHS, $p(n_S^b)$, for the interactions of ^3He and ^4He with CNO, Em and AgBr targets are displayed. In this figure, the data are compared with MCM predictions. One can observe that while the maximum experimental value of n_S^b for the interactions of the two helium isotopes with CNO nuclei equals 2, the corresponding one with AgBr nuclei equals 4. This confirms that the backward shower particles, n_S^b , are a sensitive target parameter.

As obtained earlier for the n_S^f distributions, it can be said that the agreement between n_S^b experimental data and the corresponding MCM calculations is the best for the interactions with the light CNO nuclei (Fig. 2a). However, although for interactions with Em and AgBr (Figs. 2b and c) the MCM predictions extend to higher values of n_S^b than the experimental data, it is possible to say that there is a general agreement between the experimental and theoretical results.

4.5. Multiplicity correlations

A more sensitive characteristic for the nucleus-nucleus interactions, which helps to understand the mechanism of backward particle production, is the correlation between the multiplicities of different types of emitted particles. Therefore, it is convenient to study for $^3\text{He}+\text{Em}$ and $^4\text{He}+\text{Em}$ interactions the average multiplicities of both n_S^f and n_S^b as functions of N_g^b and N_h , as well as the $\langle n_S^f \rangle$ as a function of n_S^b . These correlations are presented in Figs. 3, 4 and 5, respectively. The experimental data in these figures are compared with the corresponding MCM calculations.

a) Correlation between $\langle \mathbf{n}_S^{f,b} \rangle$ and N_g^b : The correlation between grey and shower particles is very important due to the mutual dependence of these particles on the number of struck nucleons. It can be noticed from Fig. 3a and b that both $\langle n_S^{f,b} \rangle$ linearly increase with increasing N_g^b up to 2. Such a trend could be understood from the rescattering processes occurring in the spectator parts. Starting from $N_g^b > 2$, i.e. dealing with the interactions on the heavy emulsion nuclei, the process of hadronic production is weakly connected with N_g^b . That conclusion is coming from the constant behavior of $\langle n_S^{f,b} \rangle$ at $N_g^b > 2$. It is also seen that the

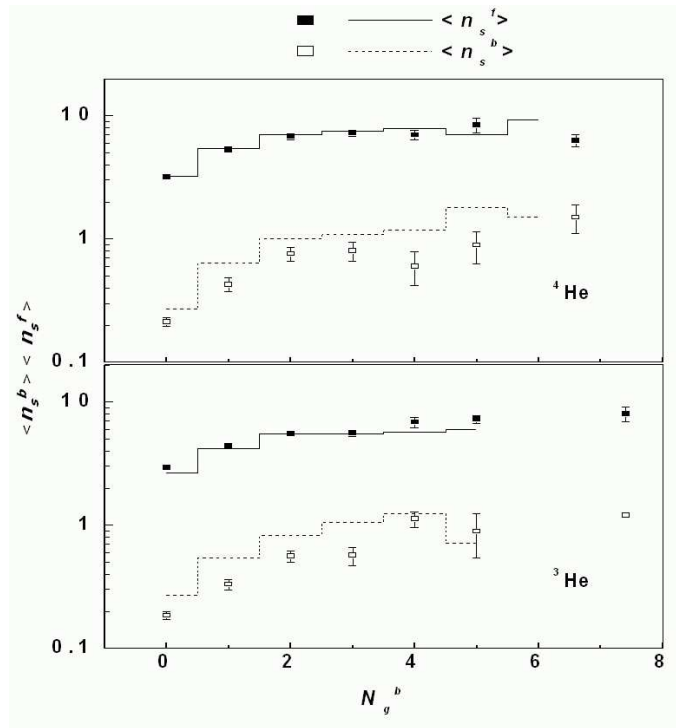


Fig. 3. The correlation between average values of forward-backward shower particles ($\langle n_s^f \rangle$ and $\langle n_s^b \rangle$) and backward grey particles (N_g^b) for the interactions of ${}^4\text{He}+\text{Em}$ (a) and ${}^3\text{He}+\text{Em}$ (b). The results with the error bars denote the experimental data and the histograms denote MCM calculations.

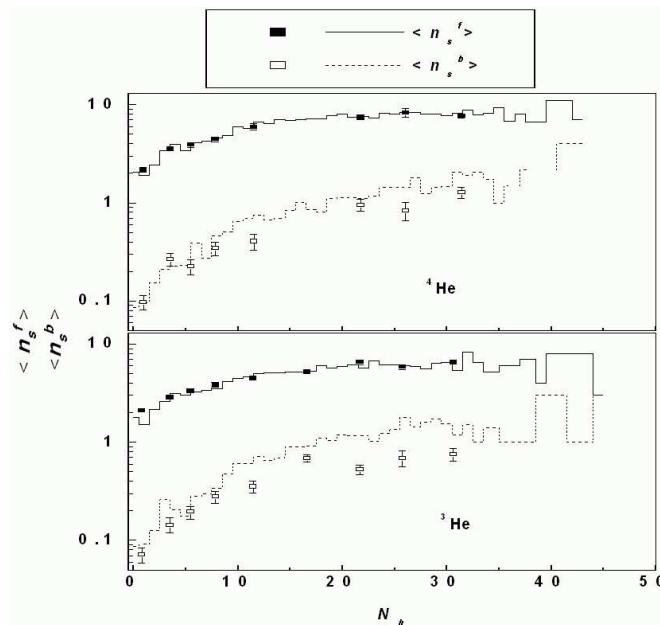


Fig. 4. The correlation between average values of forward-backward shower particles ($\langle n_s^f \rangle$ and $\langle n_s^b \rangle$) and the heavily ionizing particles N_h . The notations are identical to Fig.3.

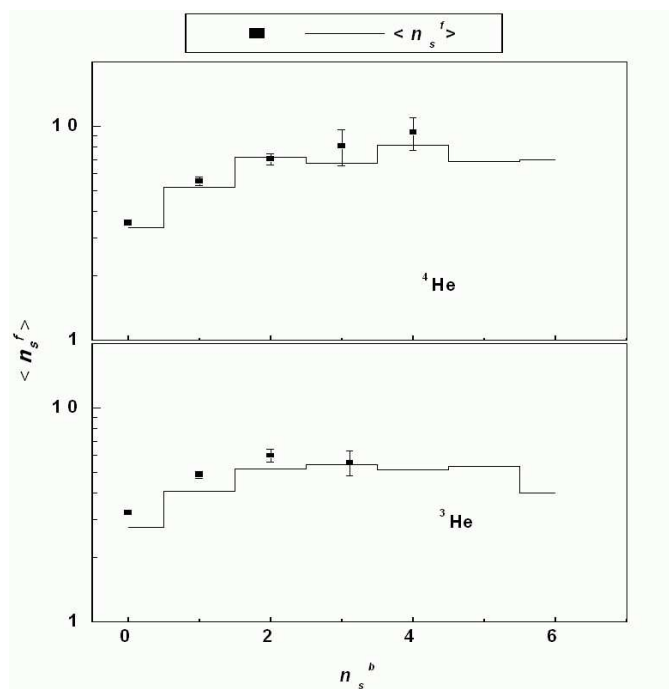


Fig. 5. The correlation between $\langle n_S^f \rangle$ and $\langle n_S^b \rangle$ for ${}^3\text{He}+\text{Em}$ and ${}^4\text{He}+\text{Em}$ interactions. The notations are the same as in Fig. 3.

MCM calculations provide a better description for the correlations between $\langle n_S^{f,b} \rangle$ and N_g^b than do the correlations between $\langle n_S^b \rangle$ and N_g^b .

b) Correlation between $\langle n_S^{f,b} \rangle$ and N_h : Experimentally, the shower particle average values ($\langle n_S^{f,b} \rangle$), shown in Fig. 4, increase with the size of the helium projectile due to the number of interacting nucleons. For the two projectiles, the figure shows that the calculated average values of the forward shower particles agree with the measured ones. Considering the backward average values, it can be seen that at $N_h \leq 8$, there is an agreement between the experimental and the calculated results, while at $N_h > 8$ the calculations exceed the experimental data.

c) Correlation between $\langle n_S^{f,b} \rangle$ and n_S^b : In Fig 5, the shower particle average values in the FHS, $\langle n_S^f \rangle$, sharply increase with increasing the number of backward shower particles up to $n_S^b \sim 2$ in the case of ${}^3\text{He}+\text{Em}$ interactions and up to $n_S^b \sim 3$ in the case of ${}^4\text{He}+\text{Em}$ ones. Beyond these limits, the average values tend to become nearly constant. The dependence of $\langle n_S^f \rangle$ on n_S^b , which is connected with helium size, seems to be in fair agreement with the predictions of MCM.

5. Conclusions

In this work, we have studied the characteristics of the backward and forward shower particle multiplicities induced in the inelastic interactions of helium isotopes (${}^3\text{He}$ and ${}^4\text{He}$) with emulsion nuclei at 3.7 AGeV. The obtained experimental

data are compared with the predictions of the modified cascade model. From the exhaustive analysis of the above data, we conclude the following:

a) The probability of the interactions accompanied by shower particles (mainly pions) flying into the BHS is about 25 % of the total interaction samples obtained for the two helium isotopes. This probability is found to increase with increasing target size, so that the number of events having $N_h > 8$ is nearly three times those characterized by $N_h \leq 8$.

b) The average shower particle multiplicities $\langle n_S^b \rangle$ produced in the interactions of ^3He and ^4He with AgBr nuclei are nearly four times higher than with the CNO nuclei.

c) The events having $n_S^b > 0$ are characterized by large values of $\langle n_S^{f,b} \rangle$.

d) The group of events having $N_h \leq 8$ and $n_S^b > 0$ can be considered as an indicator of the interactions that occur with the light target group of nuclei in the emulsion (CNO), while the events having $N_h > 8$ and $n_S^b > 0$, are due to quasi-central and central interactions with the heavy target group of nuclei (AgBr).

e) The events having $n_S^b > 0$ as well as $Q = 0$ are indicators for the occurrence of large destruction of the heavy emulsion nuclei (i.e., AgBr ones).

f) The region where $\langle n_S^f \rangle$ depends strongly on n_S^b seems to be connected with the helium size. On the other hand, the dependence of $\langle n_S^{f,b} \rangle$ on the number of backward grey particles is unaffected by the helium size.

g) The MCM-model shows an agreement with the mean values and the multiplicity distributions. However, a worse agreement between the theoretical calculations and the experimental results is observed in the reproduction interactions of the two helium isotopes with the heavy (AgBr) emulsion nuclei.

h) The MCM-model can predict the different multiplicity correlations in the low multiplicity ranges. Therefore, one can say that the MCM calculations show a good performance in describing the data produced in the region having less cascading (i.e., in the case of interactions with the CNO nuclei).

Acknowledgements

The authors gratefully thank the JINR-staff for their cooperation in supplying us with the nuclear emulsion plates. Special thanks to Prof. A. I. Malakhov and Prof. A. D. Kovalenko for their support.

References

- [1] A. M. Baldin et al., Sov. J. Nucl. Phys. **20** (1976) 629 [Yad. Fiz. 20 (1975) 1201].
- [2] L. L. Frankfurt and M. I. Strikman, Phys. Lett. B **83** (1979) 497.
- [3] C. F. Perdrisat, S. Frankel and W. Frati, Phys. Rev. C **18** (1978) 1764.
- [4] S. Nagamia et al., Phys. Rev. C **24** (1981) 971.
- [5] L. S. Schroeder et al., Phys. Rev. Lett. **43** (1979) 1787.
- [6] A. M. Baldin, Yad. Fiz. **10** (1976) 1201.

- [7] Khaled Abdel-Waged, Phys. Rev. C **59** (1999) 2792.
- [8] Tauseef Ahmed and M. Irfan, Phys. Rev. C **46** (1992) 1483.
- [9] H. B. Mathis and Meng Ta-Chung, Phys. Rev. C **18** (1978) 952.
- [10] M. El-Nadi et al., Nuovo Cimento A **111** (1998) 1243.
- [11] A. Abdelsalam et al., J. Phys. G. Nucl. Part. Phys. **28** (2002) 1375.
- [12] M. El-Nadi, A. Abdelsalam and N. Ali-Mossa, Int. J. Mod. Phys. E **3** (1994) 811.
- [13] M. El-Nadi et al., Eur. Phys. J. A **3** (1998) 183.
- [14] V. V. Burov, V. K. Lukyanov and A. I. Titov, Phys. Lett. B **67** (1977) 46.
- [15] M. I. Gorenstein and G. M. Zinovjev, Phys. Lett. B **67** (1977) 100.
- [16] EMUO1 Collaboration, M. I. Adamovich et al., Z. Phys. A **358** (1997) 337.
- [17] EMUO1 Collaboration, M. I. Adamovich et al., Phys. Lett. B **407** (1997) 92.
- [18] L. Kawrakow, M. I. Mohring and J. Ranft, Z. Phys. C **56** (1992) 115.
- [19] V. S. Barashenkov, F. G. Zheregi and Zh. Zh. Musulmanbekov, Sov. J. Nucl. Phys. **39** (1984) 715.
- [20] S. G. Mashink, In *Proceeding of a Specialist's Meeting – Intermediate Energy Nuclear Data: Models and Codes*, Paris (1994) p.107.
- [21] M. B. Blann, H. Gruppelaar, P. Nagel and J. Rodens, *International Code Comparison for Intermediate Energy Nuclear Data*, NEA, OECD, Paris (1994).
- [22] J. P. Florian et al., Phys. Rev. D **13** (1976) 558.
- [23] A. Abdelsalam, JINR, E **1** (1981) 623.

PROUČAVANJE RELATIVISTIČKE TVORBE HADRONA PREMA
 NAPRIJED I UNATRAG U SUDARIMA ^3He I ^4He S JEZGRAMA U
 EMULZIJI NA ENERGIJI UBRZIVAČA U DUBNI

Predstavljamo eksperimentalne rezultate i analize mjerenja međudjelovanja ^3He i ^4He u emulziji na $4.5 \text{ AGeV}/c$, u kojima se opažaju relativistički pljuskovi hadrona koji lete unatrag ($\theta_{\text{lab}} \leq 90^\circ$). Proučavamo ovisnost vjerojatnosti tih međudjelovanja o veličini jezgre mete, sudarnom parametru i naboju projektila-promatrača. Istražili smo prosječne vrijednosti i raspodjele višestrukosti hadrona za lake i teške jezgre u emulziji. Nadalje, proučavali smo korelacije višestrukosti različitih izlaznih čestica. Podaci pokazuju da su pljuskovi čestica unatrag osjetljiv parametar jezgri mete. Vrijednosti parametara mogu poslužiti kao dobar pokazatelj sudara s lakim odnosno teškim jezgrama. Usporedba s promijenjenim kaskadnim modelom pokazuje dobro slaganje s podacima u kojima je manje kaskada (tj. manje sudara s lakim jezgrama). Rezultati tog modela za teške jezgre veći su od eksperimentalnih podataka.